pulses to these potentials, although the spatially averaged $[Ca^{2+}]_i$ increased slowly to relatively high concentrations (Fig. 4, A and B). Calcium entry through L-type Ca^{2+} channels (V_p = −20 mV) was much more effective in triggering local $[Ca^{2+}]_i$ transients than an increase in the average $[Ca^{2+}]_i$ in the cell (V_p = +80 mV) (Fig. 4C). Local $[Ca^{2+}]_i$ transients at high positive clamp voltages were observed only in cells showing Ca^{2+} waves (*16*).

Our data support the concept that $[Ca^{2+}]_i$ transients under normal conditions (that is, without verapamil) can be explained by recruitment of more local $[Ca^{2+}]_i$ transients with the same characteristics as those observed here. First, the bell-shaped voltage dependence of the number of local $[Ca^{2+}]_i$ transients (Figs. 3B and 4B) is similar to that of the spatially averaged $[Ca^{2+}]_i$ transient (*24*), after accounting for the average $[Ca^{2+}]_i$ due to Na-Ca exchange. Second, the latency histograms are explicable in terms of the gating of L-type Ca^{2+} channels in guinea pig cardiac cells (*17*), although channel gating may be modified in the presence of verapamil (*14*). Latency histograms cannot yet be compared with measurements of whole cell SR Ca^{2+} release flux because these are not yet available for guinea pig cells. Accordingly, we determined how many local $[Ca^{2+}]_i$ transients must be evoked to produce the normal whole cell $[Ca^{2+}]_i$ transient. At 0 mV, we observed that three local $[Ca^{2+}]_i$ transients were elicited, on average, in the first 40 ms. This yields a peak frequency of ~2 s^{-1} μm^{-1} along the length of the scanned cell. As the peak average $[Ca^{2+}]_i$ is 120 nM, the contribution of each local $[Ca^{2+}]_i$ transient to the average $[Ca^{2+}]_i$ is 40 nM. Therefore, to produce a whole cell $[Ca^{2+}]_i$ transient of 1.5 μM under normal conditions, the peak frequency of local $[Ca^{2+}]_i$ transients would have to be at least 12 times greater than that observed here in the presence of verapamil. In summary, the $[Ca^{2+}]_i$ transient in the whole cell can be explained in terms of the recruitment of single, stereotyped unitary events (local $[Ca^{2+}]_i$ transients), controlled locally by single L-type Ca^{2+} channels in the plasma membrane.

REFERENCES AND NOTES

1. W. G. Wier, *Biophys. J.* **65**, 2270 (1993); E. Rios, *ibid.* **67**, 7 (1994).
2. D. J. Beuckelmann and W. G. Wier, *J. Physiol. (London)* **405**, 233 (1988); A. Fabiato, *J. Gen. Physiol.* **85**, 247 (1985).
3. A. Varro, N. Negretti, S. B. Hester, D. A. Eisner, *Pfluegers Arch.* **423**, 158 (1993); K. R. Sipido and W. G. Wier, *J. Physiol. (London)* **435**, 605 (1991).
4. L. Cleemann and M. Morad, *J. Physiol. (London)* **432**, 283 (1991).
5. W. G. Wier, T. M. Egan, J. R. López-López, C. W. Balke, *ibid.* **474**, 463 (1994).
6. M. D. Stern, *Biophys. J.* **63**, 497 (1992).
7. S. Györke and P. Palade, *Am. J. Physiol.* **264**, C1505 (1993); J. S. K. Sham, L. Cleemann, M. Morad, *Proc. Natl. Acad. Sci. U.S.A.* **92**, 121 (1995).
8. G. Isenberg and S. Han, *J. Physiol. (London)* **480**, 423 (1994).
9. J. R. López-López, P. S. Shacklock, C. W. Balke, W. G. Wier, *ibid.*, p. 21.
10. M. B. Cannell, H. Cheng, W. J. Lederer, *Biophys. J.* **67**, 1942 (1994).
11. H. Cheng, W. J. Lederer, M. B. Cannell, *Science* **262**, 740 (1993).
12. The resolution of the confocal microscope is presently not adequate to address the issue of whether calcium sparks originate from one single RyR or from a cluster of RyRs. The optical section is approximately 1 μm thick (*9*), and the point scanned is limited by diffraction at 1 μm. That means that the fluorescence represented at each pixel in the line scan is detected from a volume of approximately 1 μm^3.
13. D. Pelzer, A. Cavalié, W. Trautwein, *INSERM* **124**, 415 (1984).
14. To understand the possible relation of the local $[Ca^{2+}]_i$ transients to single L-type Ca^{2+} channel currents during clamp-pulse depolarization, it is necessary to consider how phenylalkylamines such as verapamil (and its methoxy derivative D 600) block Ca^{2+} currents. In guinea pig myocytes, D 600 reduced the mean open channel lifetime and the frequency of opening without changing the length of time until the first opening or the single-channel current amplitude (*13*). Channels could still reopen in D 600, and therefore the time course of the ensemble average current (with Ba^{2+} as the charge carrier) was not affected. Therefore, we assume that L-type Ca^{2+} channels in the presence of verapamil opened with the same first latencies, closed somewhat more quickly (0.2 ms), still reopened occasionally thereafter, and conducted the same current as control channels, but did so much less frequently (that is, the L-type open probability, $P_{o,L}$, was reduced).
15. R. A. Bouchard, R. B. Clark, W. R. Giles, *J. Physiol. (London)* **472**, 391 (1993).
16. J. R. López-López, P. S. Shacklock, C. W. Balke, W. G. Wier, unpublished data.
17. W. C. Rose, C. W. Balke, W. G. Wier, E. Marban, *J. Physiol. (London)* **456**, 267 (1992).
18. S. Györke and M. Fill, *Science* **260**, 807 (1993).
19. K. Yasui, P. Palade, S. Györke, *Biophys. J.* **67**, 457 (1994).
20. E. Carmeliet, M. Morad, G. Van Der Heyden, J. Vereecke, *J. Physiol. (London)* **376**, 143 (1986).
21. T. E. McDonald, S. Pelzer, W. Trautwein, D. J. Pelzer, *Physiol. Rev.* **74**, 365 (1994).
22. N. Leblanc and J. R. Hume, *Science* **248**, 372 (1990); W. J. Lederer, E. Niggli, R. W. Hadley, *ibid.*, p. 283; J. S. K. Sham, L. Cleemann, M. Morad, *ibid.* **255**, 850 (1992); P. Lipp and E. Niggli, *J. Physiol. (London)* **474**, 439 (1994); A. J. Levi, K. W. Spitzer, O. Kohmoto, J. H. Bridge, *Am. J. Physiol.* **266**, H1422 (1994).
23. D. J. Beuckelmann and W. G. Wier, *J. Physiol. (London)* **414**, 499 (1989).
24. W. G. Wier, *Science* **207**, 1085 (1980); L. Barcenas-Ruiz and W. G. Wier, *Circ. Res.* **61**, 148 (1987); M. B. Cannell, J. R. Berlin, W. J. Lederer, *Science* **238**, 1419 (1987); M. Näbauer, G. Callewaert, L. Cleemann, M. Morad, *ibid.* **244**, 800 (1989); W. H. duBell and S. R. Houser, *Am. J. Physiol.* **257**, H746 (1989). For a review, see D. M. Bers, *Excitation-Contraction Coupling and Cardiac Contractile Force* (Kluwer, Dordrecht, 1991).

25. Supported by U.S. Public Health Service awards HL29473 (W.G.W.), HL02466 (C.W.B.), and HL50435 (C.W.B.), an American Heart Association, Maryland Affiliate, grant-in-aid (C.W.B.), and the Division of Cardiology, Department of Medicine, University of Maryland at Baltimore, J.R.L.-L. is a Fogarty Scholar. We thank J. M. Miller for expert technical assistance in cell isolation.

7 December 1994; accepted 23 February 1995

The Control of Calcium Release in Heart Muscle

M. B. Cannell, H. Cheng, W. J. Lederer*

The control of calcium release from intracellular stores (the sarcoplasmic reticulum) in cardiac muscle was examined with the use of a confocal microscope and voltage clamp techniques. Depolarization evoked graded calcium release by altering the extent of spatial and temporal summation of elementary calcium release events called "calcium sparks." These evoked sparks were triggered by local L-type calcium channel currents in a stochastic manner, were similar at different potentials, and resembled spontaneous calcium sparks. Once triggered, the calcium release from the sarcoplasmic reticulum during a calcium spark was independent of the duration of the triggering calcium influx. These results were used to develop a unifying model for cardiac excitation-contraction coupling that explains the large (but paradoxically stable) amplification of the trigger calcium influx by a combination of digital and analog behavior.

In cardiac muscle, the archetypical ryanodine receptor (RyR) is gated by Ca^{2+} influx across the plasmalemma and serves to amplify the Ca^{2+} influx by releasing sufficient Ca^{2+} from the sarcoplasmic reticulum (SR) to activate contraction. This process is the cornerstone of excitation-contraction (EC) coupling and has been termed Ca^{2+}-induced Ca^{2+} release (CICR) (*1*). Because the Ca^{2+} efflux from the SR is between 10 and 65 times larger than that due to the Ca^{2+} current (I_{Ca}) through channels in the plasma membrane (*2*, *3*), the release of Ca^{2+} will tend to cause further release, leading to uncontrolled regenerative behavior (positive feedback). However, Ca^{2+} release from the SR seems to be tightly regulated by both the amplitude and duration of I_{Ca} (*2*, *4*, *5*). Ca^{2+}-dependent inactivation of Ca^{2+} release (*1*) could have provided a solution to this paradox; however, this mechanism has not been observed in intact cells (*4*, *6*). To

M. B. Cannell, Department of Pharmacology and Clinical Pharmacology, St. George's Hospital Medical School, Cranmer Terrace, London SW17 ORE, UK.
H. Cheng and W. J. Lederer, Department of Physiology and Medical Biotechnology Center, University of Maryland School of Medicine, 660 West Redwood Street, Baltimore, MD 21201, USA.

*To whom correspondence should be addressed.

clarify how I_{Ca} controls Ca^{2+} release from the SR, we used confocal microscopy to acquire spatially and temporally resolved images of intracellular Ca^{2+} concentration ($[Ca^{2+}]_i$), combined with whole cell voltage clamp techniques to control I_{Ca} simultaneously (*7*).

Activation of I_{Ca} normally leads to a large synchronous increase in $[Ca^{2+}]_i$ (Fig. 1A) (*8*). The $[Ca^{2+}]_i$ transient increased with a latency of 2 ms and reached 90% of its peak value in 20 ms. As reported previously, termination of the triggering I_{Ca} before the peak of the $[Ca^{2+}]_i$ transient results in a smaller $[Ca^{2+}]_i$ transient (*2*, *4*). However, the confocal microscope reveals that $[Ca^{2+}]_i$ is not spatially uniform after such a stimulus; Ca^{2+} release only takes place at a limited number of sites (Fig. 1B) that vary randomly from beat to beat. This spatial nonuniformity in $[Ca^{2+}]_i$ is not the result of the spatial organization of Ca^{2+} release sites, because the control transient (Fig. 1A) and that activated by the brief Ca^{2+} tail current (Fig. 1B), which occurs on repolarization (*2*, *4*, *9*), are much more uniform. The simplest explanation for this observation is that SR Ca^{2+} release occurs at discrete sites when a nearby Ca^{2+} channel opens (*10*), and with a short pulse, the stochastic nature of channel gating and the finite latency in the opening of the Ca^{2+} channel (*11*) result in not all release sites being activated.

As the duration of the Ca^{2+} influx is increased, the spatial averaged $[Ca^{2+}]_i$ (Fig. 2, A and B) and the rate of rise of $[Ca^{2+}]_i$ increases (Fig. 2C). The changes in the rate of rise of $[Ca^{2+}]_i$ have not been observed in earlier studies (*2*, *4*, *5*), which may be explained by the enhanced time resolution arising from the use of fluo 3 and a confocal microscope in this study. Because $[Ca^{2+}]_i$ continues to increase for about 10 ms after the cessation of I_{Ca} as shown in Fig. 2B (*12*), these results demonstrate that discrete Ca^{2+} release sites (*13*, *14*) are activated by local I_{Ca} and the termination of release is not regulated by the Ca^{2+} channel current.

The conclusion that the time-course of Ca^{2+} release is not tightly controlled by the duration of the Ca^{2+} channel current is supported by an examination of the time course of Ca^{2+} release from the SR in response to very short depolarizing pulses (~1 ms). In response to such short pulses, Ca^{2+} release often occurs at a single isolated site (Fig. 3A), thus eliminating any possible influence by the activation of adjacent SR Ca^{2+} release sites. The Ca^{2+} release occupies a region about 2 μm in diameter,

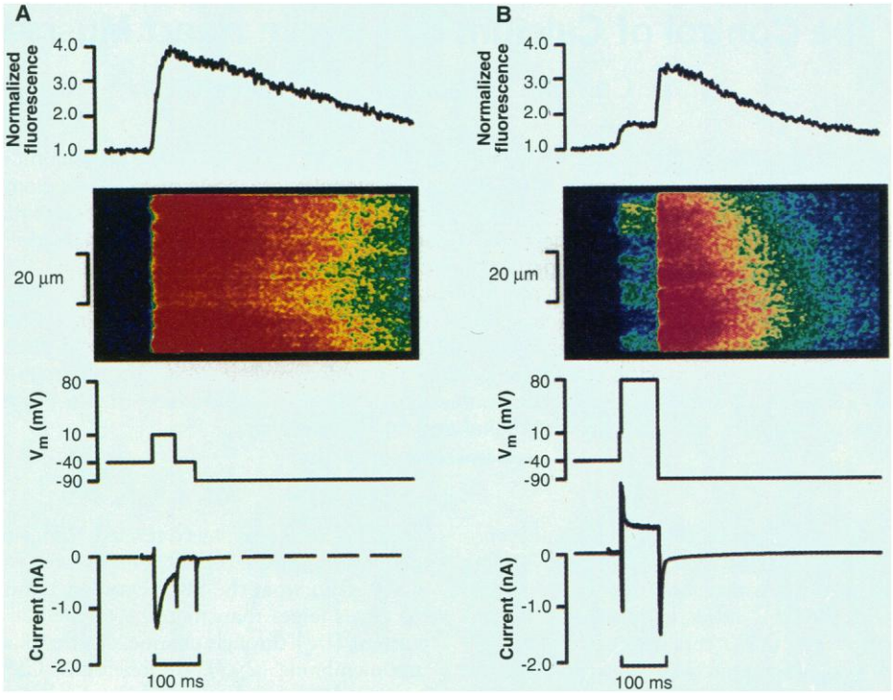

Fig. 1. Effect of depolarization duration on the uniformity of Ca^{2+} release from the SR in rat heart cells. (**A**) Confocal line-scan image of a fluo 3–loaded rat heart cell under voltage clamp. Traces show (from top to bottom) spatial average fluorescence, line-scan fluorescence image, membrane potential, and membrane current. Each line-scan image is a plot of fluorescence along a scanned line (that is, position) on the ordinate versus time (on the abscissa) (*7*). The acquisition of current data was limited to 150 ms around the depolarizing pulse to enable a high sampling frequency (the rest of the trace has been extrapolated for clarity). (**B**) Ca^{2+} transient in response to a brief period of Ca^{2+} influx. I_{Ca} was activated for 3 ms and then terminated by further depolarization to +80 mV for 80 ms. This protocol avoided the complication of a tail current, which can also evoke a large Ca^{2+} release, as seen when the cell was repolarized from +80 mV.

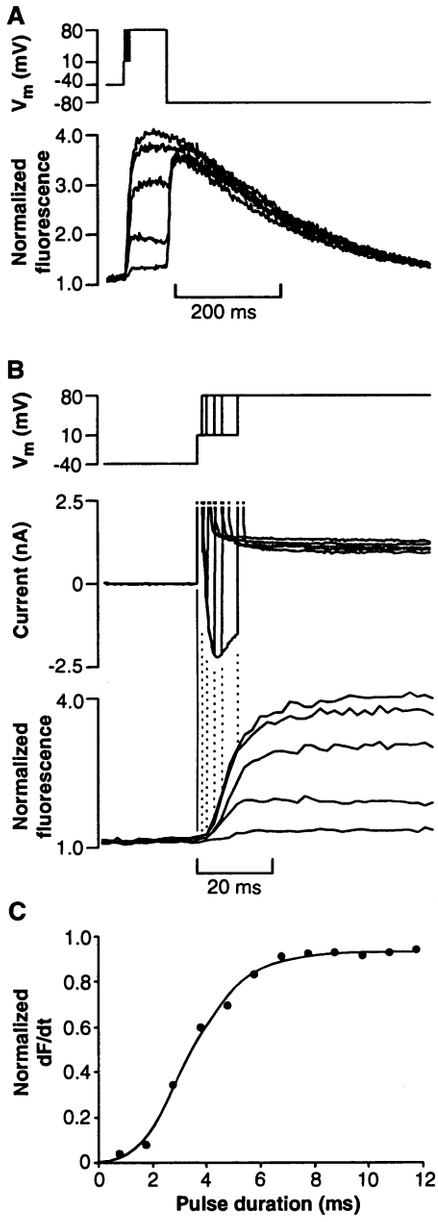

Fig. 2. Time-dependent recruitment of SR Ca release during EC coupling. (**A**) Spatially averaged $[Ca^{2+}]_i$ transients were obtained from line-scan images in response to various periods of Ca^{2+} influx. Five superimposed records are shown, indicating that for a depolarization from −40 mV to +10 mV for 1.75, 2.75, 4.75, 6.75, or 10.75 ms, the $[Ca^{2+}]_i$ transient increased from a resting fluorescence ratio of 1.0 to 1.37, 2.04, 3.17, 3.85, and 4.11, respectively. (**B**) The voltage clamp protocol and the associated Ca^{2+} currents and fluorescence records on an expanded time scale. The capacity transients associated with the step changes in membrane potential are truncated. The fluorescence record shows that the latency for the earliest release of Ca^{2+} was less than 2 ms. (**C**) The dependence of the maximum rate of change of the fluorescence record on the duration of voltage clamp pulse to +10 mV. The smooth curve through the data points was plotted by eye.

reaches its peak in about 10 ms, and declines with a half-time of ~20 ms. A small Ca^{2+} influx through I_{Ca} can also be produced by a small depolarizing pulse (to minimize the number of sarcolemmal (SL) Ca^{2+} channels opened), and this protocol (Fig. 3B) also produces a local Ca^{2+} release (*14*), albeit with a longer latency that may be explained by the low probability of Ca^{2+} channel opening at such negative potentials. These local, evoked Ca^{2+} release events have been observed over the full range of potentials (−50 to +50 mV) and are similar to "Ca^{2+} sparks" (*15*) that arise from the spontaneous gating of a "Ca^{2+} release unit" [composed of one or a small group of Ca^{2+} release channels (RyRs) (*16*)] in the SR of quiescent unstimulated cells (Fig. 3C). The similarity between spontaneous Ca^{2+} sparks and evoked local release events includes many properties such as kinetics, amplitude, and spatial size and suggests that spontaneous and evoked Ca^{2+} sparks both arise from the gating of an elementary Ca^{2+} release unit and that the number of RyRs in such an elementary unit is about the same. (*15*, *17*).

To explain both forms of behavior, we propose that the probability of evoked Ca^{2+} spark occurrence depends on the local $[Ca^{2+}]$ near the RyR release unit (*10*, *13*) and that the duration of the Ca^{2+} release during a Ca^{2+} spark is determined by the (intrinsic) gating of the SR release channels that form the release unit (*17*). The idea that local elevations of $[Ca^{2+}]$ are unable to spread regeneratively across release units under normal conditions (*18*) is supported by the observation that evoked sparks do not activate Ca^{2+} release in neighboring regions (*13*, *15*), This is due to low sensitivity of the RyR to $[Ca^{2+}]_i$ under normal conditions (*10*, *15*). It therefore follows that the stochastic recruitment of Ca^{2+} re-

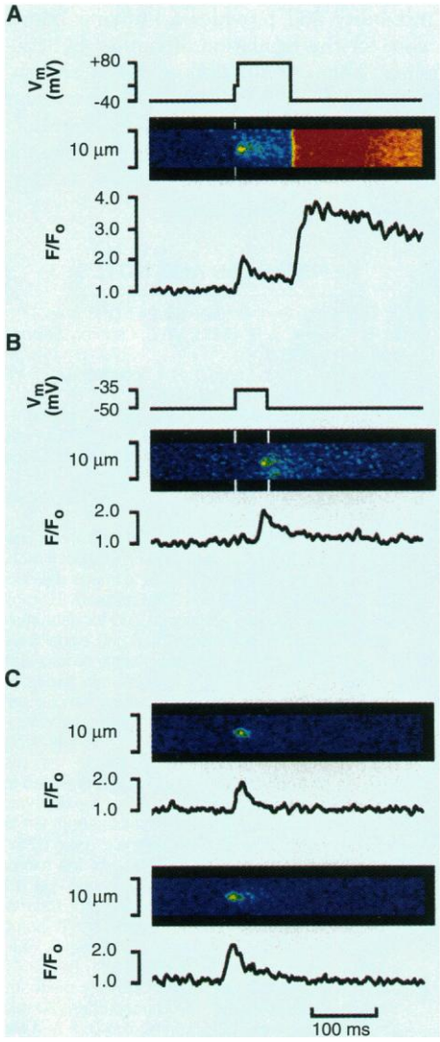

Fig. 3. Spontaneous and depolarization-activated Ca^{2+} sparks. (**A**) Depolarization from −40 mV to −5 mV for 0.75 ms activated a Ca^{2+} spark with a latency of less than 2 ms (voltage protocol was identical to that in Fig. 2). The line-scan image of the Ca^{2+} spark is shown above; the intensity of a 2-μm-wide region centered on the spark is plotted below. F/F_o is the ratio of fluorescence (F) normalized to the fluorescence under quiescent conditions (F_o) (*15*). The peak fluorescence ratio was 2.08 at 10 ms. A large uniform tail $[Ca^{2+}]_i$ transient is also observed on repolarization. (**B**) Depolarization from −50 to −35 mV activated a Ca^{2+} spark with a latency of 32 ms. The peak fluorescence ratio was 2.07 at 10 ms. (**C**) Spontaneous Ca^{2+} spark observed in a voltage-clamped ventricular myocyte held at −80 mV in the presence of 100 μM Cd^{2+} (top pair of traces; peak ratio, 1.92 at 10 ms). The bottom pair of traces shows a spontaneous Ca^{2+} spark observed in an unclamped quiescent rat ventricular myocyte loaded with fluo 3 [by the AM method (*15*)]. The peak fluorescence ratio was 2.18 at 10 ms.

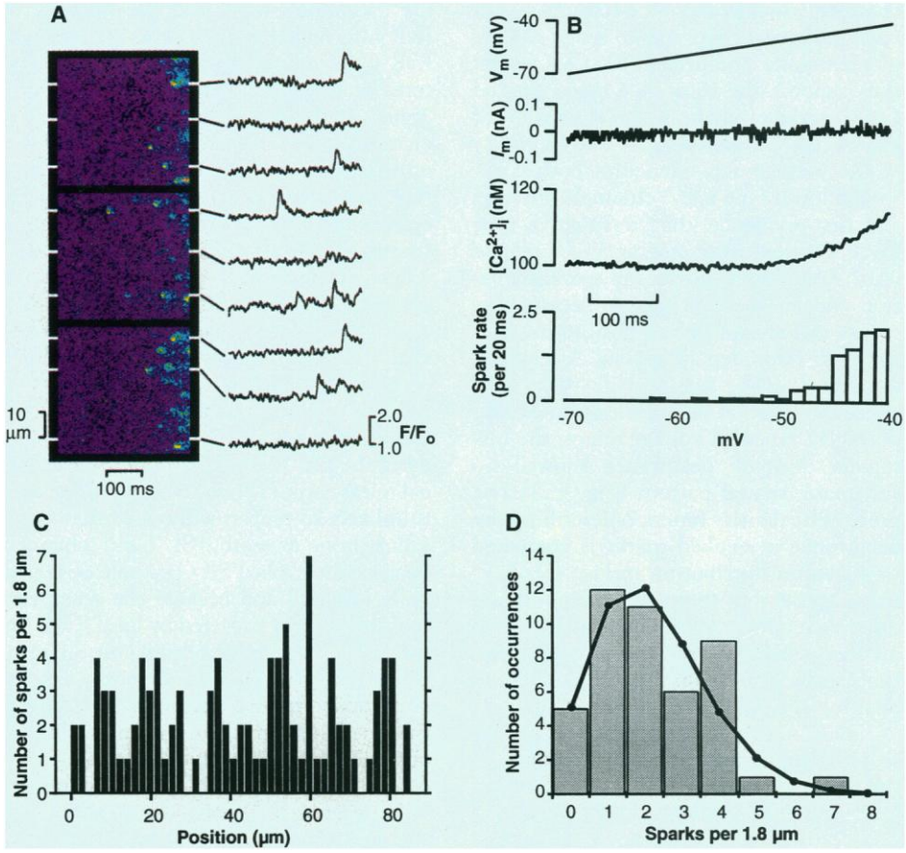

Fig. 4. Stochastic behavior of evoked Ca^{2+} sparks. (**A**) From a holding potential of −80 mV, voltage ramps to −40 mV were applied over 610 ms; the data show the range −65 mV to −40 mV. Three example line-scan images obtained during these voltage ramps are shown at the left. Representative local fluorescence traces (plotted on the right) show the amplitude and time course of the evoked sparks and no change of local $[Ca^{2+}]_i$ in nonsparking regions. (**B**) There was little change in membrane current during the ramp (top trace). Spatially averaged $[Ca^{2+}]_i$ increased slightly during the ramp depolarization (middle trace); this almost entirely resulted from the increase in spark frequency. (**C**) The occurrence of Ca^{2+} sparks in line-scan images during 12 successive ramps is plotted as a function of position (with 1.8-μm-wide histogram bins). (**D**) The data in (C) have been used to derive a probability density function for the occurrence of sparks during the ramps. The solid line superimposed on the histogram is a Poisson distribution having the same mean number of sparks per 1.8 μm (pooling the data from the 12 images gave a mean of 2.22 sparks per 1.8 μm). To examine whether these two distributions are statistically the same (hypothesis H_o), we used the χ^2 test. Because the calculated χ^2 is less than $\chi^2_{.90}$, the hypothesis H_o is accepted.

lease units during the Ca^{2+} transient must result largely from the time- and voltage-dependent opening of nearby SL Ca^{2+} channels.

If the $[Ca^{2+}]_i$ transient arises from the summation of Ca^{2+} sparks activated by the opening of single surface membrane Ca^{2+} channels, then the activation of release units should be stochastic and follow Poisson statistics when the probability of Ca^{2+} channel opening is low. To examine this point, cells were slowly depolarized from negative potentials in order to examine spark behavior around the foot of the I_{Ca} activation curve (Fig. 4A). As a cell was depolarized, the production of Ca^{2+} sparks increased exponentially, with an apparent threshold of about −55 mV, increasing e-fold in 7.5 mV (Fig. 4B). This voltage dependence is very similar to that of the activation curve of the L-type Ca^{2+} channel, which shows an e-fold change in open probability over a 6- to 8-mV change in membrane potential (*19*). Our results thus support the idea that these evoked Ca^{2+} sparks result from the activation of L-type Ca^{2+} channels (*20*). The similarity of the voltage dependence of both Ca^{2+} sparks and L-type Ca^{2+} channels provides the first evidence that a single L-type Ca^{2+} channel activates a single release unit. Visually, the pattern of spark activation appears to be stochastic because the sparks vary in timing and positioning during each ramp depolarization. After measurement of the number of sparks that occur in every 1.8 μm of the scanned line during 12 repeated voltage ramps, the histogram of spark occurrence showed no systematic spatial pattern (Fig. 4C). The probability density function describing the occurrence of evoked sparks is compared to a Poisson distribution in Fig. 4D. A χ^2 test suggests that there was no significant difference between the observed data and a Poisson process, which supports the idea that spark activation by Ca^{2+} channel opening is a stochastic process.

These results indicate that the macroscopic $[Ca^{2+}]_i$ transient can be explained by the summation of a large number of microscopic SR Ca^{2+} release events called Ca^{2+} sparks. During EC coupling, the probability of Ca^{2+} spark occurrence is greatly increased by local Ca^{2+} influx due to I_{Ca} (*21*). However, once activated, Ca^{2+} release during a Ca^{2+} spark is determined by the intrinsic gating of the SR Ca^{2+} release channels (*22*), regardless of the membrane potential and the duration of the I_{Ca}. Thus, the gradation of the whole cell $[Ca^{2+}]_i$ transient is achieved by altering the probability of Ca^{2+} spark production, rather than by modulation of the amplitude of Ca^{2+} sparks as has been previously suggested (*23*). Amplification of the trigger Ca^{2+} influx through the L-type Ca^{2+} channel during EC coupling occurs by two mechanisms (Fig. 5). The first is that the Ca^{2+} flux from activated SR release units is much greater than that due to the Ca^{2+} channel. This greater flux occurs because the conductance of the RyR is greater than that of the L-type Ca^{2+} channels (*24*), and the grouping of RyR into release units may augment single RyR Ca^{2+} efflux (*13*, *15*, *25*). These features of the release unit represent analog "gain" in the sense that the L-type Ca^{2+} channel flux is amplified by the SR release unit flux. Second, the duration of the Ca^{2+} flux from an activated SR release unit is considerably longer than the mean open time of the L-type Ca^{2+} channel. This "digital pulse stretching" behavior further increases the gain of EC coupling (*26*) but does so without introducing instability because the SR release unit eventually closes on its own. The spontaneous closure of the RyRs in a functional unit allows the high local $[Ca^{2+}]_i$ to decline rapidly in the vicinity of the Ca^{2+}-sensing sites of the individual release unit (*27*), so that the release unit is unlikely to reopen without further Ca^{2+} influx from a nearby SL Ca^{2+} channel. Because the evoked SR Ca^{2+} release is spatially localized and because the sensitivity of the unit to be triggered by local $[Ca^{2+}]$ is low (*10*, *15*), each SR release unit is largely uncoupled from its neighboring release units under normal conditions. Although these features limit the maximal gain attainable, they allow the tight and graded control of intracellular Ca^{2+} signaling (by the triggering I_{Ca}). Numerical analysis of EC coupling has shown that if all the required gain were analog, then EC coupling would be regenerative and unstable (*25*). However, the digital behavior reported here ensures that the gain inherent in the ubiquitous CICR mechanism does not result in instability and provides a unifying framework for the regulation of cardiac EC coupling. This combination of digital and analog signal transduction mechanisms may apply to other (sub)cellular signal transduction systems and provides a solution to the general problem of simultaneously achieving high gain and stability.

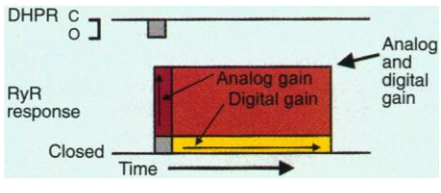

Fig. 5. Diagram illustrating how digital and analog components combine to increase amplification during EC coupling. Inward Ca^{2+} flux through the L-type Ca^{2+} channel [dihydropyridine receptor (DHPR)] triggers SR Ca^{2+} release by means of CICR. In all cases, the area under the curves shows the flux associated with the different processes; thus the ratio of areas represents gain. Analog amplification of the Ca^{2+} influx (downward deflection) through the DHPR arises from the larger efflux of Ca^{2+} from an activated SR release unit (red area). Digital gain (yellow area) arises because the mean open time of the SR Ca^{2+} release unit is longer than that of the triggering DHPR-dependent Ca^{2+} influx. The overall gain is the product of the analog and digital gain components (orange, red, and yellow areas).

REFERENCES AND NOTES

1. A. Fabiato, *J. Gen. Physiol.* **85**, 247 (1985).
2. M. B. Cannell, J. R. Berlin, W. J. Lederer, *Science* **238**, 1419 (1987).
3. W. G. Wier, T. M. Egan, J. R. López-López, C. W. Balke, *J. Physiol.* **474**, 463 (1994).
4. L. Cleeman and M. Morad, *ibid.* **432**, 283 (1991).
5. G. Callewaert, L. Cleemann, M. Morad, *Proc. Natl. Acad. Sci. U.S.A.* **82**, 2009 (1988); L. Barcenas-Ruiz and W.G. Wier, *Circ. Res.* **61**, 148 (1987).
6. M. Näbauer, and M. Morad, *Am. J. Physiol.* **258**, C189 (1990).
7. A Biorad MRC600 (Biorad, Cambridge, MA) confocal scanning head connected to a Nikon Diaphot (Nikon, New York) microscope was used to image the cells with the use of COMOS and SOM software (Biorad). IDL software (Boulder, CO) was used for data analysis. Methods for calibrating the fluo 3 signal have been described (*15*). The fluorescence record was normalized by division of the fluorescence traces by the average fluorescence during the prestimulus period. Images were acquired in the line-scan mode of the confocal microscope; this mode repeatedly scans a single line through the cell every 2 ms. The lines are plotted vertically and each line is added to the right of the preceding line to form the line-scan image. In these images, time increases from left to right and position along the scan line is given by the vertical displacement. The resolution of the microscope was approximately 0.4 × 0.4 (*x* and *y*) × 0.7 (*z*) μm. Enzymatically dissociated rat heart cells were voltage clamped with the whole cell patch clamp method [O. P. Hamill, A. Marty, E. Neher, B. Sakmann, F. J. Sigworth, *Pflueg. Arch.* **391**, 85 (1981)] with low-resistance electrodes (0.5 to 1 megohm) that were filled with 100 mM Cs aspartate, 30 mM CsCl, 10 mM Hepes, 0.1 mM K_5 fluo 3, 5 mM Mg ATP, and 10 mM NaCl (pH 7.2). The extracellular bathing solution contained 135 mM NaCl, 10 mM CsCl, 5 mM Hepes, 1.0 mM $CaCl_2$, 1.0 mM $MgCl_2$, and 10 mM glucose (pH 7.4). An Axopatch 2C and PClamp software (Axon Instruments) were used to control membrane potential and record current. Because small cells were selected and were clamped with low-resistance electrodes, the time constant of the capacitative transient was usually <300 μs, for a series resistance (after compensation) of 3 megohm. Thus the command potential would have been reached (±5%) in less than 1 ms. In all cases, similar results were obtained in at least five cells.
8. H. Cheng, W. J. Lederer, M. B. Cannell, *ibid.* **428**, 415 (1994).
9. At such positive potentials, Ca^{2+} channels are open but the driving force for Ca^{2+} entry is small. On repolarization, the driving force for Ca^{2+} entry increases greatly, so Ca^{2+} influx occurs through the open channels before they deactivate.
10. E. Niggli and W. J. Lederer [*Science* **250**, 565 (1990)] suggest in their model that SL L-type Ca^{2+} channels stochastically activate "local" or closely placed RyRs but do not directly activate either distant junctional RyRs or RyRs in the corbular SR because the RyR is relatively insensitive to $[Ca^{2+}]$.
11. W. C. Rose, C. W. Balke, W. G. Wier, E. Marban, *J. Physiol.* **456**, 267 (1992).

12. The dissipation of $[Ca^{2+}]_i$ gradients will also contribute to the time of rise of fluorescence. An artifactual increase in fura 2 (fluo 3 was used in the present study) fluorescence that lasted 10 to 20 ms has been observed during the dissipation of gradients from the surface membrane to the center of chromaffin cells 20 μm in diameter [E. Neher and G. J. Augustine, *ibid.* **450**, 273 (1992)]. We have therefore calculated whether such an effect can explain the fluorescence changes reported here. A model for Ca^{2+} binding and buffering reactions that fits the time course of the evoked $[Ca^{2+}]_i$ transient has been presented elsewhere [C. W. Balke, T. M. Egan, W. G. Wier, *ibid.* **474**, 447 (1994)], and the appropriate equations describing diffusion from a point source were added. The changes in fluo 3 fluorescence associated with a Ca^{2+} spark for Ca^{2+} release fluxes of 4 pA (for 10 ms), 40 pA (for 1 ms), and 400 pA (for 0.1 ms) were then calculated. These fluxes resulted in similar peak normalized fluorescence (1.82, 1.93, and 1.91, respectively, averaged over a 2-μm region), but the rise times were quite different, peaking in 10.0, 1.6, and 1.1 ms, respectively. We conclude that the observed rise time of the fluorescence record cannot be explained by the dissipation of $[Ca^{2+}]_i$ gradients and therefore reflects the duration of SR Ca^{2+} release.
13. M. B. Cannell, H. Cheng, W. J. Lederer, *Biophys. J.* **67**, 1942 (1994).
14. Pharmacologically reducing the probability of SL Ca^{2+} channel opening also reduces the uniformity of the $[Ca^{2+}]_i$ transient in a way that is consistent with the idea that EC coupling is locally regulated by Ca^{2+} influx through Ca^{2+} channels (*13*) [M. B. Cannell, H. Cheng, W. J. Lederer, *J. Physiol.* **477**, 25P (1994); H. Cheng, M. B. Cannell, W. J. Lederer, *Circ. Res.* **76**, 236 (1995)]. Recently, it has been shown that alterations in I_{Ca} amplitude (by depolarization to different potentials) can also lead to spatial nonuniformity in $[Ca^{2+}]_i$(*23*), which further supports the idea that it is the local Ca^{2+} influx that determines the probability of activation of SR Ca^{2+} release.
15. H. Cheng, W. J. Lederer, M. B. Cannell, *Science* **262**, 740 (1993).
16. G. Meissner, *J. .Biol. Chem.* **261**, 6300 (1986); E. Rousseau, J. S. Smith, G. Meissner, *Am. J. Physiol.* **253**, C364 (1987).
17. The amplitude of the spontaneous Ca^{2+} spark could be explained by a number of SR release channels acting in concert as the conductance of a single RyR is barely sufficient to supply the calculated SR release flux (*15*). Several other lines of evidence suggest that SR release channels may be grouped together (*13*, *25*) in a functional unit. In skeletal muscle, anatomical evidence suggests that the RyRs may be clustered in the terminal cisterns of the SR [D. G. Ferguson, H. W. Schwartz, C. Franzini-Armstrong, *J. Cell Biol.* **99**, 1735 (1984)], whereas biochemical measurements indicate that the numbers of SL Ca^{2+} channels are insufficient to individually control RyRs (in cardiac myocytes) [D. M. Bers and V. M. Stiffel, *Am. J. Physiol.* **264**, C1587 (1993)]. If this is the case, the release of Ca^{2+} during a Ca^{2+} spark could be the result of the activation of a number of SR release channels acting in concert (*15*), which would then make up the release unit (*13*).
18. S. C. O'Neill, J. G. Mill, D. A. Eisner, *ibid.* **258**, C1165 (1990); A. W. Trafford, S. C. O'Neill, D. A. Eisner, *Pflueg. Arch.* **425**, 181 (1993).
19. T. F. McDonald, S. Pelzer, W. Trautwein, D. J. Pelzer, *Physiol. Rev.* **74**, 365 (1994).
20. The Na-Ca exchanger may stimulate SR Ca^{2+} release [N. Leblanc and J. R. Hume, *Science* **248**, 372 (1990); P. Lipp and E. Niggli, *J. Physiol.* **474**, 439 (1994)]. However, the voltage dependence of Na-Ca exchange {70 mV per e-fold change [E. Niggli and W. J. Lederer, *Nature* **349**, 621 (1991)]} does not match the observed voltage dependence of the spark rate. In addition, application of 100 μM Cd^{2+} (which blocks the I_{Ca}) prevents evoked Ca^{2+} sparks during the ramp depolarization.
21. At rest, the rate of spark production is about 1 s^{-1} in a line-scan image (*15*). Because a Ca^{2+} spark rate of 2.0 per 20 ms (Fig. 4) gives a spatial average increase in $[Ca^{2+}]_i$ of 17 nM at the end of the voltage ramp, we estimate that a Ca^{2+} transient of 1 μM would require an increase in Ca^{2+} spark rate of ~ 6 × 10^3 s^{-1}. If the probability of SR release channel opening is proportional to the square of the local $[Ca^{2+}]_i$ [S. Györke and M. Fill, *Science* **260**, 807 (1993)], then this increase in rate suggests that the local trigger $[Ca^{2+}]_i$ would be ~77 times the resting $[Ca^{2+}]_i$ or about 8 μM. Such high $[Ca^{2+}]_i$ will only occur close to open channels (*27*), so that all the channels within a release unit may be activated whereas those further away are not. Given this insensitivity of the RyR for $[Ca^{2+}]_i$ this calculation can also explain why a Ca^{2+} spark does not normally propagate (*15*) and suggests that the release unit is only effectively triggered by the local Ca^{2+} influx through a nearby SL Ca^{2+} channel.
22. Even at high local $[Ca^{2+}]_i$, SR release channels eventually close. This results from their intrinsic gating (note that their open probability must be <1). The mean open time of a release unit will depend on the physical organization of the channels in the unit (*25*) and on other factors that may influence the channel gating, such as phosphorylation state [H. H. Valdivia, G. Ellis-Davies, J. Kaplan, W. J. Lederer, *ibid.* **267**, 1997 (1995).
23. J. R. López-López, P. S. Shacklock, C. W. Balke, W. G. Wier, *J. Physiol.* **480**, 21 (1994)
24. Under near-physiological ionic conditions, the SR release channel current is about 2.2 pA [E. Rousseau and G. Meissner, *Am. J. Physiol.* **256**, H328 (1989)], whereas the SL Ca^{2+} channel's current is about 0.3 pA (*11*, *19*).
25. M. D. Stern, *Biophys. J.* **63**, 497 (1992).
26. The total flux associated with a channel opening is the single channel current multiplied by its open time. Our modeling and data suggest that the duration of Ca^{2+} release from a release unit is longer than the mean open time of a SL Ca^{2+} channel [<1 ms (*11*)]. Although Ca^{2+} release from an SR release unit is triggered by the opening of a SL Ca^{2+} channel, the release unit does not require the maintained presence of the SL Ca^{2+} influx because while it is open, the release within the unit is self sustaining (or regenerative). This regenerative behavior contributes to the release unit being open for a longer period of time than the SL Ca^{2+} channel (Fig. 5). We call this effect digital pulse stretching, by analogy with the use of monostables in digital electronics to produce longer pulses than their triggers. However, although regenerative, the release is not uncontrolled because the finite open time of the release unit effectively breaks the regenerative feedback loop.
27. We calculate that the local $[Ca^{2+}]_i$ 20, 80, and 180 nm from an open SR release channel (4 pA of Ca^{2+} flux) would be about 56, 18, and 7.7 μM, respectively. This local $[Ca^{2+}]_i$ would decay by half in 4.8, 211, and 765 μs, respectively, after channel closure. Thus the probability of a second channel in the release unit opening will depend on its distance from the first channel and will rapidly decline after closure of the first channel (*25*). The high local $[Ca^{2+}]_i$ needed to trigger the release unit comes from a nearby SL Ca^{2+} channel. However, because of the low conductance of SL Ca^{2+} channels (*24*), the Ca^{2+} channel that triggers a release unit must be even closer (within ~20 nm) to a RyR in the unit.
28. Supported by grants from NIH (HL36974 and HL25675), by Directed Research Initiative Funds awards from the Medical Biotechnology Center of the University of Maryland at Baltimore, and by the British Heart Foundation, London, UK.

31 October 1994; accepted 6 March 1995

Identification of hSRP1α as a Functional Receptor for Nuclear Localization Sequences

Karsten Weis, Iain W. Mattaj, Angus I. Lamond*

Import of proteins into the nucleus is a two-step process, involving nuclear localization sequence (NLS)–dependent docking of the substrate at the nuclear envelope followed by translocation through the nuclear pore. A recombinant human protein, hSRP1α, bound in vitro specifically and directly to substrates containing either a simple or bipartite NLS motif. hSRP1α promoted docking of import substrates to the nuclear envelope and together with recombinant human Ran reconstituted complete nuclear protein import. Thus, hSRP1α has the properties of a cytosolic receptor for both simple and bipartite NLS motifs.

Import of proteins into the nucleus is an active process consisting of at least two steps: first, the energy-independent docking of the substrate to the nuclear envelope, and second, translocation through the nuclear pore complex, which requires energy (*1*). The presence of a specific NLS in the imported protein is a prerequisite for both steps. In most cases the NLS consists either of a short domain of basic amino acids—for example, the simple NLS of SV40 T antigen (PKKKRKV)—or of two stretches of basic residues separated by a spacer of about 10 amino acids, the bipartite NLS motif (*2*).

A variety of biochemical and genetic approaches have been used to search for factors involved in nuclear protein import (*3*). Biochemical fractionation of import activities, by means of an in vitro transport assay (*4*), has shown that the two steps of nuclear protein import can be mimicked by two cytosolic fractions, A and B (*5*). Fraction B mediates the translocation step and consists of two protein components, Ran/TC4 and pp15 (*6*–*8*). Recently, importin has been identified as a *Xenopus* factor required for the first step of nuclear import (*9*). Importin is homologous to the yeast protein SRP1 (suppressor of RNA polymerase 1) (*10*). Factors that bind to the NLS motif in vitro are likely to play an important role in the import reaction. Such NLS-binding factors could either be free cytosolic proteins or could be associated with the nuclear envelope. Sever-

European Molecular Biology Laboratory, Meyerhofstrasse 1, Postfach 102209, D-69012 Heidelberg, Germany.

*To whom correspondence should be addressed.